

# Neuronal Subclass-Selective Loss of Pyruvate Dehydrogenase Immunoreactivity Following Canine Cardiac Arrest and Resuscitation

Yolanda E. Bogaert,<sup>\*,1</sup> Kwan-Fu Rex Sheu,<sup>†,2</sup> Patrick R. Hof,<sup>‡</sup> Abraham M. Brown,<sup>†</sup> John P. Blass,<sup>†</sup> Robert E. Rosenthal,<sup>\*</sup> and Gary Fiskum<sup>\*,3</sup>

*\*Departments of Biochemistry and Molecular Biology and Emergency Medicine, George Washington University School of Medicine, Washington, DC 20031; †Burke Medical Research Institute, Cornell University Medical College, White Plains, New York 10605; and ‡Kastor Neurobiology of Aging Laboratories and Fishberg Research Center for Neurobiology, and Departments of Geriatrics and Adult Development, and Ophthalmology, Mount Sinai School of Medicine, New York, New York 10029*

Received December 28, 1998; accepted September 16, 1999

**Chronic impairment of aerobic energy metabolism accompanies global cerebral ischemia and reperfusion and likely contributes to delayed neuronal cell death. Reperfusion-dependent inhibition of pyruvate dehydrogenase complex (PDHC) enzyme activity has been described and proposed to be at least partially responsible for this metabolic abnormality. This study tested the hypothesis that global cerebral ischemia and reperfusion results in the loss of pyruvate dehydrogenase immunoreactivity and that such loss is associated with selective neuronal vulnerability to transient ischemia. Following 10 min canine cardiac arrest, resuscitation, and 2 or 24 h of restoration of spontaneous circulation, brains were either perfusion fixed for immunohistochemical analyses or biopsy samples were removed for Western immunoblot analyses of PDHC immunoreactivity. A significant decrease in immunoreactivity was observed in frontal cortex homogenates from both 2 and 24 h reperfused animals compared to samples from nonischemic control animals. These results were supported by confocal microscopic immunohistochemical determinations of pyruvate dehydrogenase immunoreactivity in the neuronal cell bodies located within different layers of the frontal cortex. Loss of immunoreactivity was greatest for pyramidal neurons located in layer V compared to neurons in layers IIIc/IV, which correlates with a greater vulnerability of layer V neurons to delayed death caused by transient global cerebral ischemia.** © 2000 Academic Press

**Key Words:** cardiac arrest; cerebral ischemia; laser scanning microscopy; mitochondria; neocortex; reperfusion.

## INTRODUCTION

Delayed neuronal death following transient global cerebral ischemia and reperfusion occurs by both necrosis and apoptosis. Mitochondrial dysfunction has been strongly implicated in mediating both forms of neuronal death (1, 2, 25). Alterations in mitochondrial oxidative phosphorylation, Ca<sup>2+</sup> transport, free radical generation, release of apoptotic factors, and metabolic enzymes contribute to oxidative stress, cellular Ca<sup>2+</sup> overload, activation of cell death proteases, and metabolic failure (8).

Using a clinically relevant canine model of cardiac arrest and resuscitation, we have demonstrated a chronic exacerbation of anaerobic cerebral energy metabolism that is related to neurological outcome (33). Although studies on ischemic alterations of mitochondrial oxidative energy metabolism have focused on alterations in electron transport chain activities (1, 9, 31), observations indicating a postischemic hyperoxidation of pyridine nucleotides and electron transport chain components have suggested that a deficiency in the generation of reducing power to be used by the electron transport chain may be just as important (27, 30). Consistent with these observations are the findings by several laboratories that reperfusion causes a significant decrease in the maximal activity of brain pyruvate dehydrogenase complex (PDHC), which catalyzes the critical oxidation/reduction reaction that links glycolysis to the tricarboxylic acid cycle (5, 11, 18, 46–48).

Abnormally low levels of PDHC have also been associated with chronic neurodegenerative disorders including Alzheimer's disease (35), Huntington's disease (43), Wernicke–Korsakoff syndrome (20), and a variety of hereditary ataxias (37). Although a sufficient reduction in PDHC activity could lead to metabolic failure, oxidative stress, and cell death, no direct cause and effect relationships have been established. One

<sup>1</sup> Present address: University of Colorado Health Science Center, Denver, CO 80262.

<sup>2</sup> Deceased.

<sup>3</sup> Present address: Department of Anesthesiology, University of Maryland, Baltimore School of Medicine, Baltimore, MD 21201.

approach that would aid in establishing this relationship would be to compare the pattern of inhibition of PDHC among neuronal subclasses with the selective vulnerability of neuronal subtypes to acute or delayed death.

The mechanism responsible for reduced PDHC activity in animal models and many human disorders is, at this juncture, unknown. However, *in vitro* studies have suggested that inhibition could be due to either oxidation of critical sulfhydryl groups (45) or metal-catalyzed site-specific oxidation of any one of a number of susceptible amino acids (5). Site-specific protein oxidation has been observed in some but not all models of cerebral ischemia and reperfusion (10, 19, 21, 26), in Alzheimer's disease (42), during normal aging, and in various models of neurotoxicity, such as paraquat toxicity, magnesium deficiency, and chronic exposure to alcohol (4). Oxidative damage to proteins is also promoted by conditions known to exist following cerebral ischemia, e.g., low pH (12), as well as high  $\text{Ca}^{2+}$  in the case of PDHC (5). Evidence suggests that this mechanism of inhibition is responsible for the reduction in brain glutamine synthetase activity following global ischemia (26). Studies also indicate that site-specific oxidation of this and many other proteins results in an increased rate of proteolytic degradation, as detected by a decrease in immunoreactivity (44). The present study was conducted to determine if the immunoreactivity of PDHC is reduced in the cerebral cortex following cardiac arrest and resuscitation and to determine if the pattern of reduction matches the relative vulnerability of cortical neuronal subclasses to delayed death.

## MATERIALS AND METHODS

### *Global Cerebral Ischemia and Reperfusion*

All experiments were performed in accordance with the guidelines of the Institutional Animal Use and Care Committee of the George Washington University. A canine model of cardiac arrest and resuscitation as a clinically relevant model for global cerebral ischemia and reperfusion has been described (32, 33). Adult female beagles weighing 10–15 kg were initially anesthetized with thiamylal sodium and prolonged anesthesia was induced by infusion of  $\alpha$ -chloralose (75 mg/kg). Animals were endotracheally intubated and ventilated with room air prior to induction of cardiac arrest. Muscle paralysis was maintained with i.v. pancuronium bromide and antibiotic prophylaxis was administered with ceftriaxone. Resuscitative drugs were administered via a venous catheter advanced to the level of the right atrium. Arterial pressure was continuously monitored through a femoral arterial catheter. Pulse, ECG, and rectal temperature were also continuously monitored and the temperature maintained at between 37 and 39°C by lights and heating blankets.

A thoracotomy was performed on all animals, including nonarrested controls. Ventricular fibrillation cardiac arrest was induced with a train of electrical current applied directly to the epicardium of the right ventricle following incision and reflection of the pericardium. Artificial respiration was discontinued at the onset of fibrillation. Following 10 min of cardiac arrest, animals were either sacrificed or cardiopulmonary resuscitation (CPR) was initiated to allow for reperfusion periods of either 2 or 24 h. Resuscitation was initiated by open chest cardiac massage, administration of epinephrine and sodium bicarbonate, and ventilation with 100%  $\text{O}_2$ . Open chest CPR was continued for 3 min at a rate of 50/min followed by internal defibrillation. Arterial blood gas samples were measured prior to arrest, 2 min following defibrillation, and frequently thereafter. The ventilator was adjusted following the first blood gas determination and thereafter to maintain arterial  $\text{pO}_2$  between 80 and 100 mm Hg and  $\text{pCO}_2$  between 25 and 35 mm Hg. Artificial ventilation was maintained for 22 h, at which time dogs were weaned from controlled ventilation. Animals were maintained under constant intensive care and were presumed to be subject to postoperative pain, which was controlled using a constant infusion of morphine sulfate at 1 mg/h throughout the experiments.

### *Tissue Acquisition*

Biopsy samples for immunoblot analyses were obtained from the frontal cortex of chloralose-anesthetized animals following a craniotomy and immediately prior to euthanasia with 0.25 ml/kg Euthanasia-6 (Veterinary Labs, Lenexa, KS). These samples were immediately immersed in liquid nitrogen and stored at  $-75^\circ\text{C}$ . For immunohistochemistry, dogs were perfused transcardially with ice-cold 1% paraformaldehyde in phosphate-buffered saline (PBS, pH 7.4) for 1 min followed by cold 4% paraformaldehyde in PBS for 10–15 min at a flow rate of 300 ml/min as previously described (15–17). After perfusion, the brains were immediately removed from the skull.

### *Immunoblot Measurements*

Polyclonal antibodies against bovine PDHC were raised as described previously (34). Antibodies specific for PDHC components were raised against the respective bovine proteins that were excised from SDS-polyacrylamide gels. Samples of frozen frontal cortex (approximately 0.2 g wet wt) that had been stored at  $-75^\circ\text{C}$  were weighed and homogenized with a Brinkman Polytron homogenizer in a medium previously described for use in enzyme activity measurements (5). The ice-cold medium (9 ml/g sample) contained 50 mM potassium phosphate buffer (pH 7.8), 1 mM EDTA, and 0.1% (wt/vol) Triton X-100. The protein concentration of

the homogenate was determined by a modified Biuret procedure (41). Brain proteins were resolved on 10% SDS-polyacrylamide gels (1 mm thick) by electrophoresis and then electrotransferred to nitrocellulose membranes for 3–4 h at 5 V/cm in a Bio-Rad Transblot Cell with plate electrodes (Bio-Rad Laboratories, Hercules, CA). These conditions were optimized for detection of the  $\alpha$ E1p and E2p components of the PDHC. The electrotransfer of  $\alpha$ E1p was variable, and under these conditions,  $\beta$ E1p passed through the membrane and was detected poorly. For Western blotting analysis, the membranes were preincubated with a blocking buffer containing 150 mM NaCl, 50 mM Tris-HCl (pH 7.6) and 0.05% Tween 20 (TBST), and 2% bovine serum albumin (Sigma, St. Louis, MO) and then incubated for 2 h with the anti-PDHC antibody diluted 1:1200 in the blocking buffer. After three rinses with TBST, the membranes were probed for 2 h with the  $^{125}$ I-labeled goat anti-rabbit IgG secondary antibodies (Amersham Life Science, Arlington Heights, IL) diluted in TBST at a concentration of 3  $\mu$ Ci/100 cm<sup>2</sup> of membrane. The blots were rinsed six times with TBST and the bound radioactive antibody was detected with a Phosphorimager (Molecular Dynamics, Sunnyvale, CA). The abundance of  $\alpha$ E1p and E2p for each sample was quantified by integration of the total phosphorimager signal for that band. A standard box was used for all bands, which were completely enclosed by this box. Background values were measured in an adjacent region of the same lane using the standard box and were subtracted from the integrated band intensity. Variations in labeling and transfer efficiency between blots were corrected by normalization of sample signals to a standard sample included on each blot.

### Immunohistochemistry

Perfusion fixed brains were blocked into coronal sections that included the frontal cortex area 8a in the gyrus preureus and postfixed in 4% paraformaldehyde for an additional 6 h (15–17). Following postfixation, coronal blocks to be used in immunofluorescence studies were transferred to a PBS buffer and sectioned on a vibratome at 20  $\mu$ m within 2 days of fixation. All other blocks were frozen on dry ice after cryoprotection in a graded series of PBS-buffered sucrose solutions and sectioned on a cryostat at 40  $\mu$ m. All sections from each block were kept in anatomical series and every 10th section was processed for immunohistochemistry. The remaining sections were stored in serial order at  $-20^{\circ}$ C in a cryoprotection solution consisting of glycerol, ethylene glycol, distilled H<sub>2</sub>O, and PBS (3:3:3:1 volume ratio). The sections were incubated for 48 h at  $4^{\circ}$ C with the primary antibodies in PBS containing 0.3% Triton X-100 and 0.5 mg/ml bovine serum albumin. Following incubation, the sections were processed by the avidin-biotin method using a Vectastain ABC kit (Vector

Laboratories, Burlingame, CA) and 3,3'-diaminobenzidine as a chromogen and intensified in osmium tetroxide. For double labeling fluorescence studies, sections were incubated simultaneously for 2 h with relevant secondary antibodies conjugated to Texas-Red (TR) or to fluorescein isothiocyanate (FITC). A fully characterized, specific rabbit polyclonal antibody to PDHC was used at a working dilution of 1:1000 (24, 35, 36). A mouse monoclonal antibody to the microtubule-associated protein (MAP2) was used to visualize the neuronal and dendritic organization of the dog neocortex (Sigma, St. Louis, MO; working dilution: 1:3000). A parallel series of sections was stained with cresyl violet to clarify cytoarchitecture.

Sections double labeled for PDHC and MAP2 were analyzed using a Zeiss 410 laser scanning confocal microscope (LSM, Zeiss, Oberkochen, Germany). This system includes a Zeiss Axiovert inverted microscope, an Ar/Kr laser, a PC computer and optical disk storage device. Optical densities of labeling were assessed quantitatively according to the paradigm developed by Gazzaley *et al.* (13). Sections were initially screened under epifluorescence using a 10 $\times$  Zeiss Plan-Neofluar objective and filters selective for visualizing FITC or TR to select areas of interest. The area selected was then viewed through a Zeiss 63 $\times$ /1.25 NA Plan-Neofluar objective for analysis. Images were digitized on the computer display as sections were scanned with an Ar/Kr laser, whose wavelength was specific to the excitation of the fluorescent marker (i.e., 488 nm for FITC and 568 nm for TR), reflected to the specimen by an FT488/568 dichroic mirror and a 90% neutral density filter attenuation. A contrast/brightness setting was determined for each marker, yielding high-resolution images for both bright and dim zones of the sections without regions where pixel intensity reached saturation. Images were subsequently enlarged, yielding a final magnification of 189 $\times$ , to clearly delineate cell boundaries. Several serial optical planes of section within a neuron were analyzed for level of immunolabeling to determine an average intensity/area for a given neuron. This is especially important in the case of large pyramidal neurons where some of the fluorescence may lie out of focus on a single optical plane of section. The soma of the neuron in layers III/IVc and V were then traced and their ratio of fluorescence intensity/area was recorded. Since PDHC is exclusively present in mitochondria, the unstained nuclei were chosen to determine the amount of background staining which was subtracted from the intensity of the staining in the perikaryon. The intensity/area of the nucleus was determined in order to ensure that the level of background staining was comparable among sections. Subtraction of background fluorescence was used to establish a pixel intensity threshold below which a pixel would not contribute to the average pixel intensity (or

area) of the field, thus delineating precisely the specific neuronal area to be quantified (13). Twenty to 30 neurons per layer and per section were analyzed using at least five sections per animal. Comparative data analysis used one-way ANOVA and the Duncan's method for multiple pairwise comparisons.

## RESULTS

### *Canine Cerebral Cortex Pyruvate Dehydrogenase Immunoreactivity*

Previous experiments suggested that the reperfusion-dependent reduction in canine cerebral cortex PDHC activity could be due to site-specific protein oxidation (5). As this form of oxidative injury has been shown to mark proteins for proteolytic degradation (44), we tested the hypothesis that PDHC immunoreactivity is reduced following cerebral ischemia and reperfusion due to cardiac arrest and resuscitation. Figure 1A describes a representative PDHC immunoblot, using different amounts of frontal cortex homogenate protein to establish the relationship between levels of protein and immunoreactivities as quantified with phosphorimager signals obtained from the blots. The antibodies raised against bovine PDHC recognized canine brain

PDHC proteins and the electrophoretic mobilities of the canine proteins were similar to those observed previously for bovine proteins (34). The identities of the E2p (72 kDa),  $\alpha$ E1p (41 kDa), and  $\beta$ E1p (34 kDa) proteins were also verified with antibodies specific for each of the individual proteins (data not shown). The phosphorimager signals for both E2p and  $\alpha$ E1p were linearly related to the quantity of homogenate protein within at least the range of 2–11  $\mu$ g protein (Fig. 1B). The signal for  $\beta$ E1p was relatively weak and therefore no attempts were made to quantify this signal.

Comparisons of PDHC immunoblots for frontal cortex homogenates obtained from nonischemic control animals (C), animals following 10 min cardiac arrest-induced ischemia, and animals that were reperfused for 2 or 24 h following 10 min ischemia are described in Fig. 2. Figure 2B shows a representative immunoblot and Fig. 2A presents the average levels of  $\alpha$ E1p and E2p immunoreactivity ( $\pm$ SEM,  $n = 4$ ) for the experimental groups normalized to levels found in the nonischemic control tissue. Although there appears to be a slight reduction in both  $\alpha$ E1p and E2p immunoreactivity following ischemia alone, this was not statistically significant. There was, however, a significant reduction of approximately 45% in  $\alpha$ E1p reactivity and a 30–35%

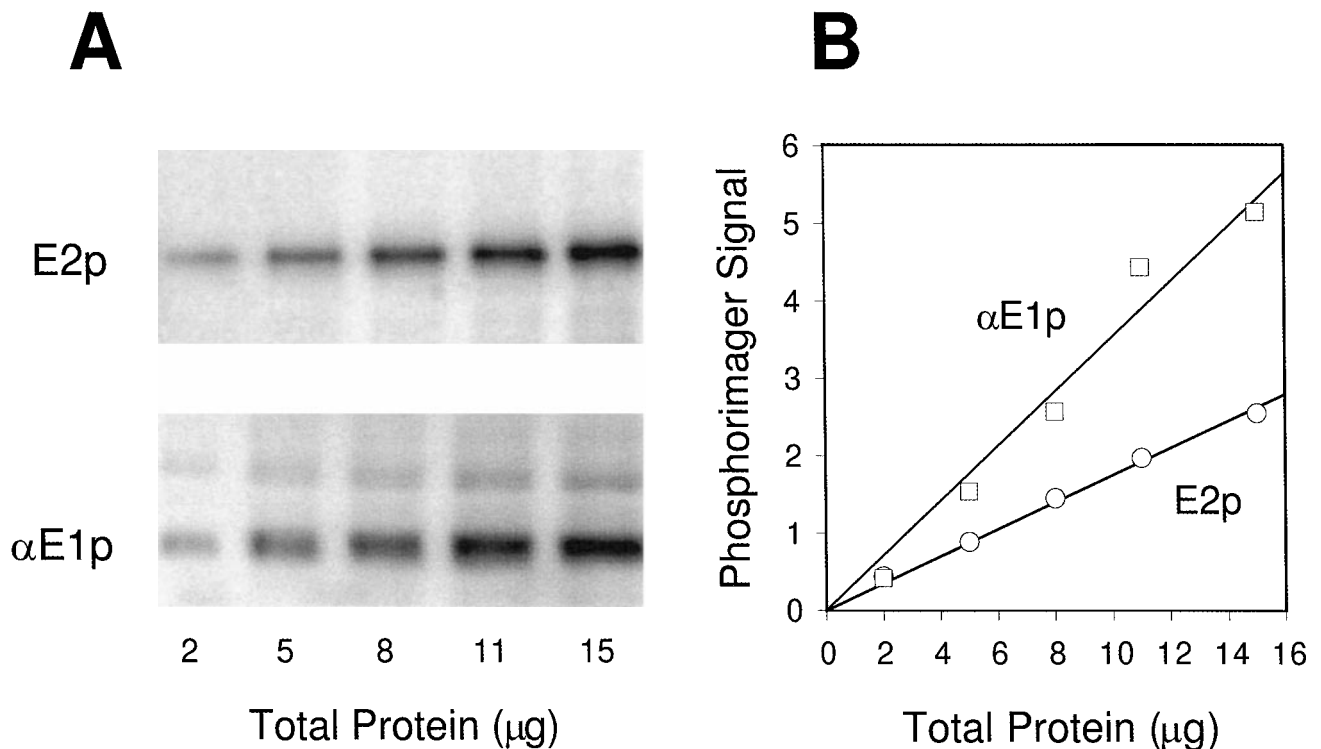


**FIG. 1.** Western blot analysis of PDHC proteins in canine frontal cortex. Immunoreactivities were developed with  $^{125}$ I-labeled secondary antibodies and quantified with a phosphorimager. (A) Immunoblot showing  $\alpha$ E1p and E2p at loaded levels of cortical homogenate protein ranging from 2 to 15  $\mu$ g. (B) The relationship of phosphorimager signals for  $\alpha$ E1p and E2p (in arbitrary units) compared to the amount of homogenate protein analyzed in blots such as that shown in A. Linear regression analysis shows  $r^2 = 0.974$  and  $0.998$  for  $\alpha$ E1p and E2p, respectively.

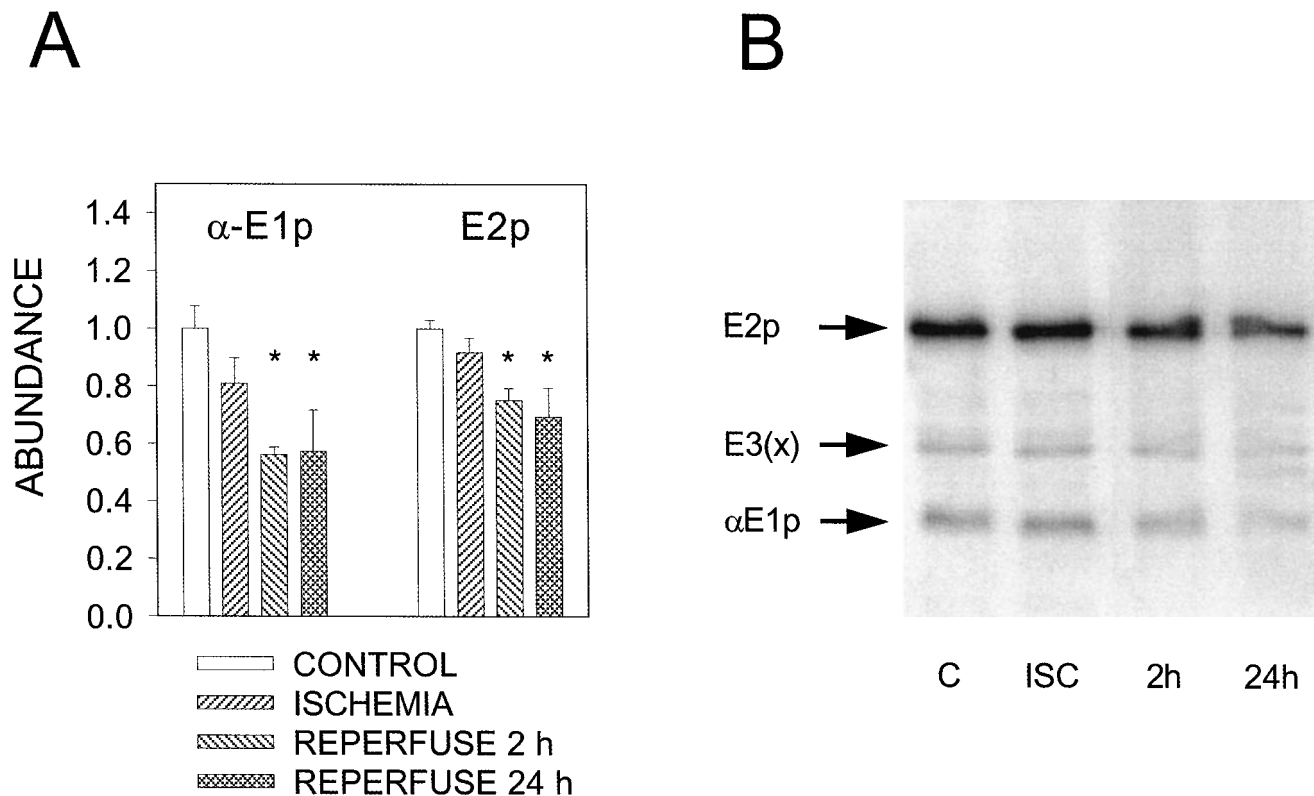


**FIG. 2.** Western blot determination of PDHC  $\alpha$ E1p and E2p immunoreactivities in canine frontal cortex samples from control (C), 10 min ischemic (ISC), and 2 or 24 h reperused animals (2 h, 24 h). (A) Mean immunoreactivity normalized to control samples ( $\pm$ SEM) for four animals per experimental group. \*, Statistically significant difference from Control ( $P < 0.05$ ). (B) Representative immunoblot including a control sample as a standard of reference.

reduction in E2p reactivity following ischemia plus either 2 or 24 h reperfusion ( $P < 0.05$ ).

#### *Cytochemical Localization of PDHC Immunoreactivity within the Frontal Cortex of Control, Ischemic, and Reperused Brains*

Given the finding that immunoreactivity of PDHC proteins  $\alpha$ E1p and E2p is reduced in homogenates of canine frontal cortex following 10 min ischemia plus as little as 2 h reperfusion, cell-selective distribution of PDHC was measured throughout layers of the frontal cortex that are known to exhibit variable sensitivity to postischemic neuronal death. The dorsal anterior prefrontal cortex, corresponding to area 8a on the gyrus proraus, was characterized by a dense Nissl-staining layer II that contained high numbers of small pyramidal neurons and a layer III with relatively larger and sparser pyramidal neurons (Fig. 3A). The distinction between the deep portion of layer III (IIIc) and layer IV was difficult to establish on Nissl-stained materials due to the rather poor definition of layer IV. Layer IV appeared as a thin zone predominantly composed of relatively small granular neurons intermingled with layer IIIc that was characterized by the occurrence of

pyramidal neurons. Layer V was easily distinguished and had much larger pyramidal neurons than layer IIIc. Layer VI was much more heterogeneous and contained small pyramidal and fusiform neurons (Fig. 3A; 15).

In control animals, strong PDHC immunoreactivity was observed in the neurons of layer III and predominantly in large pyramidal neurons of layer V, whereas smaller neurons tended to be less intensely labeled (Figs. 3B and 4A). MAP2 immunoreactivity revealed the neuronal characteristics of the different cortical layers with a prominent staining of large pyramidal neurons in layers IIIc and V. The small pyramidal neurons in layer II appeared as a dense band of MAP2 immunoreactivity, and the layer VI polymorphic neurons were intensely stained. Also, the dendritic arbor of all neuron types was remarkably labeled by the anti-MAP2 antibody and the presence of dendritic bundles was observed throughout the cortical thickness (Fig. 3C).

Pyruvate dehydrogenase is exclusively localized to mitochondria, which are present to varying extents in all brain cells. Mitochondria are predominantly located in presynaptic nerve endings and in neuronal cell

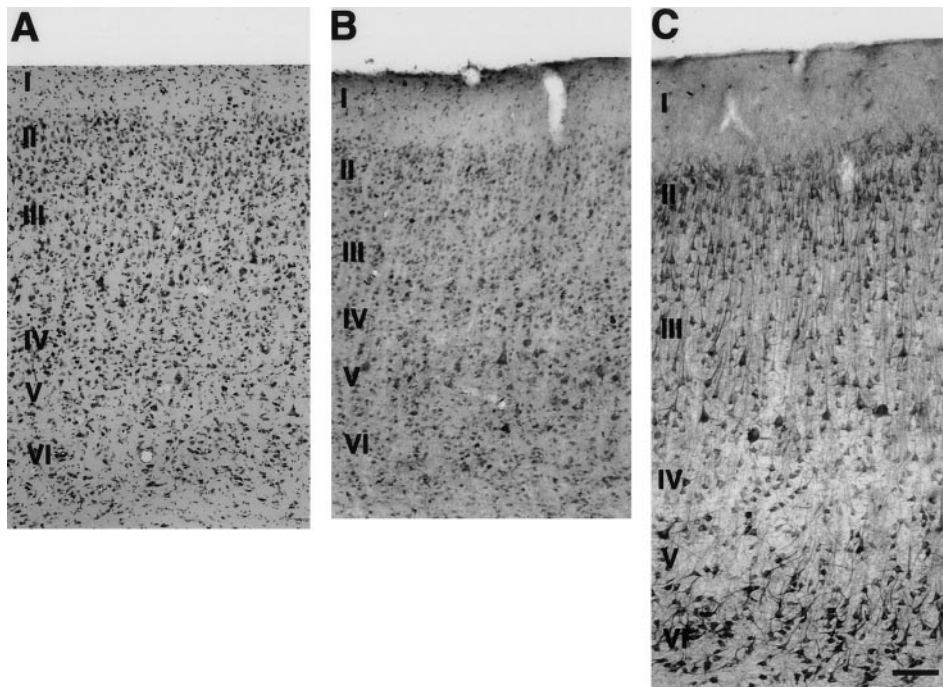


**FIG. 3.** Cytoarchitecture of area 8a in the frontal cortex of a nonischemic dog. (A) Nissl stain shows a dense layer II and the presence of pyramidal cells in layers III and V. Layer IV is poorly differentiated and layer VI contains a polymorphic population of neurons. (B) In sections incubated with a polyclonal antibody to PDHC, staining is observed primarily in medium to large neurons in layers III and V, while smaller neurons are less intensely stained. (C) MAP2 immunoreactivity is observed in most neuronal types and reveals the dendritic arborization of pyramidal cells. Cortical layers are indicated by Roman numerals. Scale bar (on C) = 100  $\mu$ m.

bodies but can also be found to a lesser extent in axons. Brightfield microscopy examination of DAB-treated materials revealed a global decrease in staining intensity at 2 and 24 h reperfusion compared to control animals and dogs with 10 min ischemia (Fig. 4). It is worth noting that after 10 min ischemia, no major changes were observed in the staining intensity compared to that seen under the control condition and that, in particular, the large layer IIIc and layer V pyramidal neurons exhibited a morphology comparable to that in control animals (Figs. 4A and 4B). A gradual decrease in intensity of PDHC immunolabeling was observed at 2 and 24 h reperfusion, although discerning differences in staining intensity among neuronal subtypes is difficult at low magnification. At higher magnification (Fig. 5), it is clear that 2 h reperfusion resulted in a relatively selective loss of immunostaining in large pyramidal neurons within layer V vs layer IIIc/IV and that the small neurons appeared to be less affected.

Laser scanning confocal microscopy analysis at even higher magnification showed that immunofluorescent staining of PDHC in layer V of the frontal cortex displays a punctate or thread-like pattern within both the cell soma and neuropil that is consistent with the known distribution of mitochondria (Fig. 6A). Although little, if any, change in layer V PDHC immunostaining was apparent following 10 min ischemia alone (Fig.

6B), there was a striking reduction in the immunostaining of both the pyramidal cell soma and surrounding neuropil in layer V following either 2 or 24 h reperfusion (Figs. 6C and 6D). The reduction in immunostaining following 2 h reperfusion cannot be explained by widespread necrosis. Although approximately 30% of layer V pyramidal neurons appear necrotic at 24 h reperfusion (6), essentially no evidence of cell death is present within any cortical layers at 2 h reperfusion in this model or other models of transient global cerebral ischemia. Moreover, robust MAP2 immunostaining of cell bodies and dendritic processes was present throughout the cortical layers at 2 h reperfusion (Fig. 6E). In contrast to the reduction in PDHC immunostaining observed in the large pyramidal cells of layer V following 2 to 24 h reperfusion, immunostaining of the relatively small neurons present within layer IIIc and in the thin layer IV was preserved following 2 h reperfusion (see Fig. 6F, which shows layer IIIc/IV in a double-labeled section using TR to stain PDHC and FITC to stain MAP2; primary colocalization was in the neuron soma, verifying the neuronal enrichment of PDHC).

A quantitative assessment of PDHC immunofluorescence was conducted using laser scanning confocal microscopy in order to provide further evidence for a reperfusion-dependent and neuronal subclass-selective

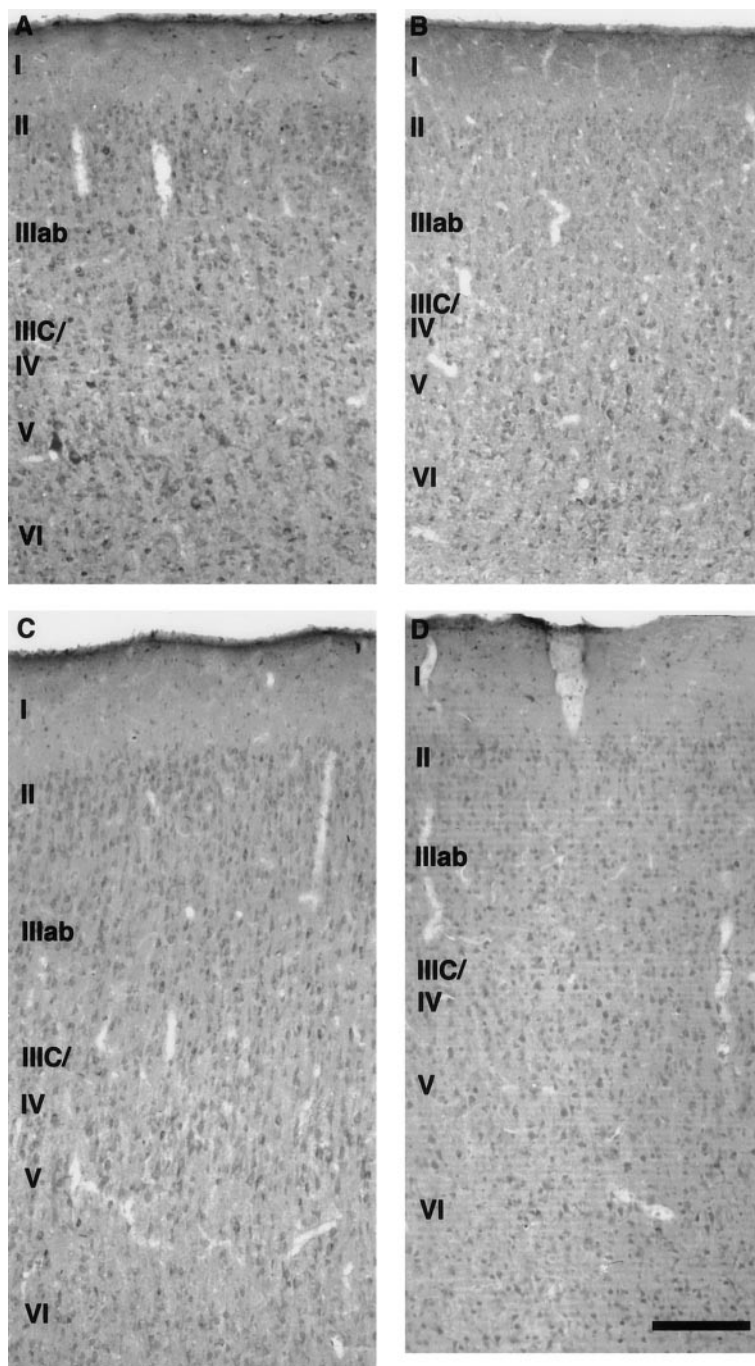


**FIG. 4.** Low magnification photomontages of area 8a in the dog frontal cortex showing the laminar distribution of PDHC immunoreactivity in a control animal (A), following 10 min ischemia alone (B), and after 2 h (C) and 24 h (D) reperfusion. Note the decrease in staining intensity in the 24-h reperfusion animal compared to that seen in the other conditions. However, at this level of resolution, subtle laminar differences in PDHC staining intensity and the involvement of particular neuronal populations are not reliably detectable, whereas they are clearly visible at higher magnification. Cortical layers are indicated by Roman numerals. Scale bar (on D) = 160  $\mu\text{m}$ .

reduction in PDHC immunoreactivity. The results summarized in Table 1 represent data collected from two animals per group, using five sections per animal and measuring 20–30 neurons per cortical layer and section. Although no reduction in the immunofluorescence

per unit area of layer V neuronal cell bodies was evident following ischemia alone, a significant, approximately 50% reduction was apparent following 2 h reperfusion ( $P < 0.05$ ). In contrast, no reduction in immunofluorescence per unit area was observed in the

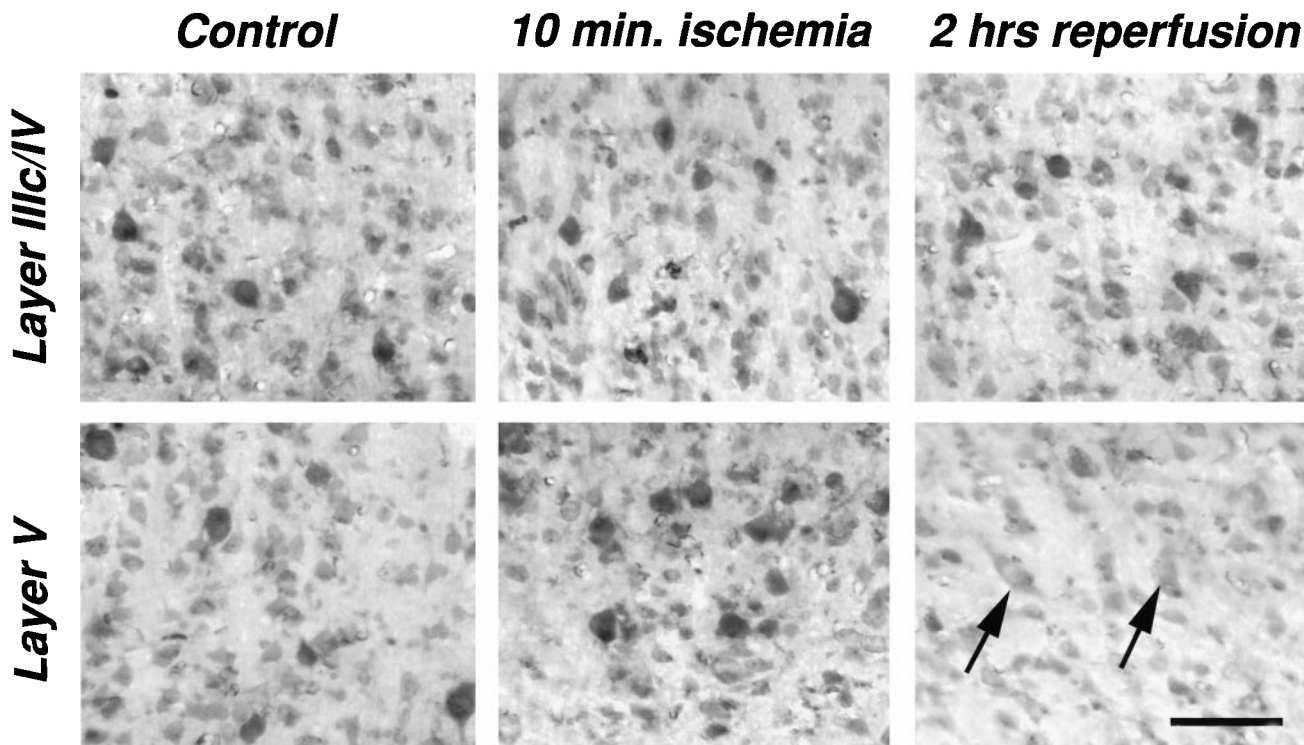


**FIG. 5.** PDHC immunoreactivity in layer IIIc/IV (top row) and in layer V (bottom row) of a control dog (left column), following 10 min of ischemia (middle column), and following 2 h of reperfusion (right column). Note the presence of large, intensely stained neurons in both layers in all conditions except in layer V of the 2-h-reperfusion animal. In this case large layer V neurons exhibit a considerably lighter staining (arrows). Compare with Table 1. Scale bar = 75  $\mu$ m.

neuronal cell bodies located in layers IIIc–IV following either 10 min ischemia or 2 h reperfusion. In order to control for possible differences in staining of different specimens, the ratio of immunofluorescence for cells in layer V compared to cells in layers IIIc/IV within individual sections were obtained and are summarized in Table 1. No reduction in the ratio of fluorescence between the two areas was observed following ischemia alone. However, a significant reduction was observed following 2 h reperfusion ( $P < 0.05$ ).

#### DISCUSSION

A reperfusion-dependent decrease in brain pyruvate dehydrogenase activity has been reported for several different models of cerebral ischemia (5, 11, 18, 46, 47). Using the canine cardiac arrest model, we observed a profound, 40–70% inhibition of PDHC activity in canine frontal cortex following 30 min to 24 h reperfusion (5). The results of the present study using the same model indicate that the reduction in activity in brain tissue homogenates is at least qualitatively related to the reduction in PDHC immunoreactivity ( $\alpha$ E1p and E2p) following both 2 and 24 h reperfusion. Ten minutes ischemia alone resulted in no loss of immunoreactivity, which is consistent with the lack of an effect of

ischemia alone on PDHC maximal enzyme activity (5). The reperfusion-dependent loss of PDHC immunoreactivity is in contrast to the finding of Zaidan *et al.* (48), who used a rat four-vessel occlusion model of global cerebral ischemia and observed no loss of PDHC immunoreactivity. However, the rat model differs from the canine model in several respects. In the rat model, although PDHC activity is reduced in the relatively vulnerable dorsolateral striatum, PDHC activity appears unchanged in the cerebral cortex (48). The extent of inhibition of PDHC activity in the rat striatum is also considerably less than the inhibition we have observed in the canine cortex (5). Also, the spatial and temporal pattern of neuronal injury in cardiac arrest compared to arterial occlusion models of global cerebral ischemia is somewhat different (29).

The mechanism by which PDHC is inhibited during reperfusion may provide a further explanation for the uncoupling between PDHC enzyme activity and immunoreactivity. We have previously postulated that reperfusion-dependent inhibition of PDHC activity may be due to site-specific protein oxidation (5). Others have suggested that inactivation is specifically due to sulfhydryl oxidation (45). Site-specific protein oxidation does not necessarily result in an immediate loss of immunoreactivity but does appear to mark the targeted pro-

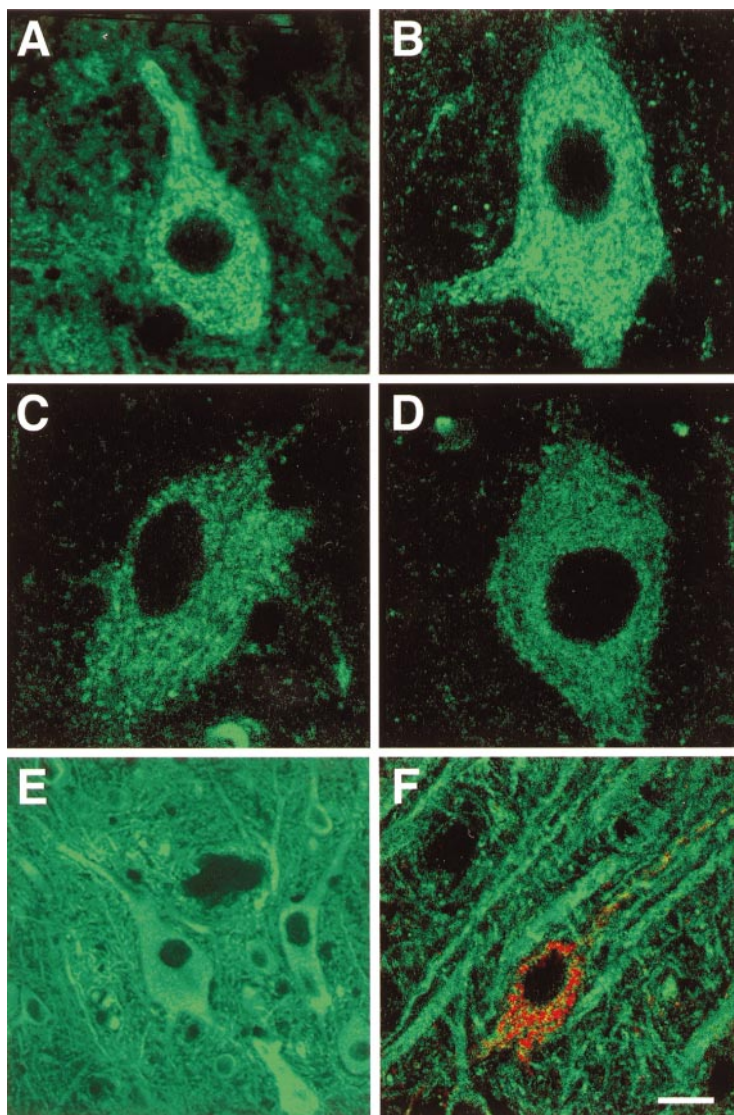


**FIG. 6.** Confocal imaging of PDHC (A–D and F) and MAP2 (E, F) in the frontal cortex of control and experimental dogs. Cortical layer V PDHC immunoreactivity in control (A) and 10-min-ischemic (B) tissues appears similar, while immunofluorescence in both the cell soma and neuropil appears reduced in both 2-h (C)- and 24-h (D)-reperused animals. Robust somatic and dendritic MAP2 immunostaining was present in layers IIIc/IV (E, F) and in layer V (not shown) following ischemia and 2 h reperfusion. (F) Robust PDHC staining (red) in a MAP2-staining neuron (green) in layers IIIc/IV following 2 h reperfusion. Scale bar in A–D and F = 12  $\mu\text{m}$  and in E = 30  $\mu\text{m}$ .

teins for proteasomal degradation (44). It is likely that the susceptibility to degradation is dependent upon the extent of protein oxidation. Therefore, although a given oxidative insult may be sufficient to inactivate an enzyme, it may not be sufficient to result in proteolytic degradation. This possibility could help explain why the reduction in PDHC  $\alpha\text{E}1\text{p}$  and particularly  $\text{E}2\text{p}$  immunoreactivity is not as great as the reduction in PDH activity that we have previously reported (5). The fact that we observed a greater loss of PDHC activity in a model where site-specific protein oxidation is known to exist (21) than was observed by Zaidan *et al.* (48) could also explain the difference in the effects of ischemia/reperfusion on PDHC immunoreactivity observed in these two systems.

The finding that PDHC immunoreactivity was altered during cerebral ischemia and reperfusion allowed for comparisons between the levels of PDHC in neurons present in different layers of the frontal cortex that exhibit different vulnerabilities to ischemic cell death. Typically, relatively large neurons in the middle of cortical layer III and throughout layer V exhibit the greatest vulnerability to delayed death, with neurons in layers I, IV, and VI being more resistant to injury (28). The relative susceptibility of different neuronal subclasses to ischemic injury is multifactorial and probably dependent on the degree to which these cells undergo and withstand  $\text{Ca}^{2+}$  overload, oxidative stress, and metabolic failure (8, 40). We decided to compare

TABLE 1

Quantitative Laser Scanning Confocal Analysis of PDHC Immunoreactivity in Canine Neocortex Following Ischemia/Reperfusion

Animal group	Layer V	Layer IIIc/IV	Ratio V:IIIc/IV
Control	107.2 ± 6.8	79.4 ± 2.8	1.35 ± 0.04
10 Min ischemia	106.0 ± 16.0	78.5 ± 3.5	1.34 ± 0.15
2 H reperfusion	55.4 ± 3.4*	82.5 ± 4.5	0.68 ± 0.08*

*Note.* Results represent the means ± SEM of immunofluorescence intensity per unit area as described under Materials and Methods. Data were obtained using two animals per group and five frontal cortex sections per animal. Immunofluorescence was measured for the cell bodies of 20–30 neurons per section, yielding 200–300 measurements per group. The ratio of fluorescence for layers V:IIIc/IV was determined for individual sections, yielding 10 measurements per group.

\* Significantly different from the control group ( $P < 0.05$ ).

the pattern of PDHC levels in layers IIIc/IV compared to that in layer V to test the hypothesis that a reduction in the level of this important enzyme in cerebral energy metabolism is a prelethal marker of susceptibility to delayed death. The neuronal somata of these particular layers were chosen due to the relative ease of identification and demarcation and due to the fact that significantly greater delayed neuronal death is apparent in layer V than in layer IV (i.e., our layer IIIc/IV) in both rat and canine models of global cerebral ischemia (28, 39, and P. Hof, unpublished observations).

The finding that the level of PDHC in either neuronal subclass was unchanged following ischemia alone is consistent with the results of the western immunoblots, and consistent with the lack of inhibition of PDHC activity reported previously (5). The observation that PDHC immunoreactivity in cortical layer V neuronal cell bodies was reduced by approximately 50% following 2 h reperfusion is consistent with both the Western immunoblot measurements and with enzyme activity measurements performed on frontal cortex homogenates. Although PDHC immunoreactivity was reduced following 2 h reperfusion in the neuropil as well as in the cell bodies within cortical layer V, there was no reduction in PDHC staining intensity in the cell bodies located within layers IIIc/IV. This finding was verified by independently measuring the ratio of immunofluorescence per unit area for cell soma in layer V versus layers IIIc/IV, since the ratio of fluorescence for the two areas within individual sections should be unaffected by variations in staining between samples. The observation that there was a significant decrease in this ratio following 2 h reperfusion but not following 10 min ischemia alone is consistent with the immunofluorescence measurements performed on individual neurons present in different sections from different perfusion

fixed specimens. It is therefore concluded that 10 min cardiac arrest and 2 h reperfusion results in a reduction in PDHC immunoreactivity that is relatively specific for large pyramidal neurons present in layer V compared to the smaller neurons present in layers IIIc/IV of the canine neocortex.

The selective, prelethal loss of PDHC in the cortical layer V pyramidal cells is consistent with the relative vulnerability of these neurons in this and other models of global cerebral ischemia and reperfusion (28, 39). Although these results do not establish a cause-and-effect relationship between the loss of PDHC and neuronal death, they do support the hypothesis that the reduction in PDHC is a sensitive molecular marker of irreversible neuronal injury. If, as we and others have postulated, the reperfusion-dependent loss of PDHC activity is due to one or more forms of oxidative injury (5, 45), the reduction in PDHC levels may serve as a marker of differential sensitivity to oxidative stress. It should therefore be determined if the loss of PDHC is related to histochemical indicators of oxidative stress, e.g., products of protein oxidation and lipid peroxidation products, and whether such relationships are evident within different neuronal subclasses.

In addition to the possible relationship between PDHC levels and oxidative stress, it is likely that some cells lose sufficient PDHC activity to severely impair the production of reduced pyridine nucleotides that could limit production of ATP by oxidative phosphorylation. A shift in metabolism toward anaerobic glycolysis caused by impaired PDHC activity would promote chronic lactic acidosis and alter other metabolic pathways that are dependent on normal tricarboxylic acid cycle activity, such as neurotransmitter biosynthesis. Any or all of these sequelae could easily contribute to the pathogenesis of ischemic cell death. In addition to the correlative results described in the present study, support for the involvement of altered PDHC activity in ischemic neurodegeneration comes from animal experiments demonstrating neuroprotection by agents that either stimulate PDHC activity, such as dichloroacetate (7, 18), or metabolic substrates that bypass the PDHC step to generate acetylCoA, such as 1,3-butanediol (22, 14) and acetyl-L-carnitine (3, 23, 33, 38). It remains to be determined to what extent PDHC levels and PDHC activity must be reduced to actually precipitate or potentiate neuronal death and whether pharmacological agents directed at counteracting PDHC inhibition are therapeutically effective in human ischemic brain disorders.

#### ACKNOWLEDGMENTS

We thank A. P. Leonard for expert technical assistance. This work was supported by NIH Grants NS34152 and AG09014 and by Sigma Tau, S.p.A.

## REFERENCES

1. Abe, K., M. Aoki, J. Kawagoe, T. Yoshida, A. Hatori, K. Kogure, and Y. Itoyama. 1995. Ischemic delayed neuronal death—A mitochondrial hypothesis. *Stroke* **26**: 1478–1489.
2. Ankarcrone, M., J. M. Dypbukt, E. Bonfoco, B. Zhivotovsky, S. Orrenius, S. A. Lipton, and P. Nicotera. 1995. Glutamate-induced neuronal death: A succession of necrosis or apoptosis depending on mitochondrial function. *Neuron* **15**: 961–973.
3. Aureli, T., A. Miccheli, M. E. DiCocco, O. Ghirardi, A. Giuliani, M. T. Ramacci, and F. Conti. 1994. Effect of acetyl-L-carnitine on recovery of brain phosphorus metabolites and lactic acid level during reperfusion after cerebral ischemia in the rat—Study by <sup>31</sup>P- and <sup>1</sup>H-NMR spectroscopy. *Brain Res.* **643**: 92–99.
4. Berlett, B. S., and E. R. Stadtman. 1997. Protein oxidation in aging, disease, and oxidative stress. *J. Biol. Chem.* **272**: 30313–20316.
5. Bogaert, Y. E., R. E. Rosenthal, and G. Fiskum. 1994. Post-ischemic inhibition of cerebral cortex pyruvate dehydrogenase. *Free Rad. Biol. Med.* **16**: 811–820.
6. Bogaert, Y. E., A. Levesque, P. R. Hof, Y. Haywood, R. E. Rosenthal, and G. Fiskum. 1996. Postischemic ventilatory O<sub>2</sub> influences neurological, histological and neurochemical outcome following canine cardiac arrest. *Soc. Neurosci. Abstr.* **22**: 2148.
7. Chang, L. H., H. Shimizu, H. Abiko, R. A. Swanson, A. I. Faden, T. L. James, and P. R. Weinstein. 1992. Effect of dichloroacetate on recovery of brain lactate, phosphorus energy metabolites, and glutamate during reperfusion after complete cerebral ischemia in rats. *J. Cereb. Blood Flow Metab.* **12**: 1030–1038.
8. Fiskum, G. 1997. Metabolic failure and oxidative stress contribute to ischemic neurological impairment and delayed cell death. In *Neuroprotection* (T.J.J. Blanck, Ed.), pp. 1–22. Williams and Wilkins, Baltimore, MD.
9. Fiskum, G., A. N. Murphy, and M. F. Beal. 1999. Mitochondria in neurodegeneration: Acute ischemia and chronic neurodegenerative diseases. *J. Cereb. Blood Flow Metab.* **19**: 351–369.
10. Folbergrova, J., Y. Kiyota, K. Pahlmark, H. Memezaqa, M. L. Smith, and B. K. Siesjö. 1993. Does ischemia with reperfusion lead to oxidative damage to proteins in the brain? *J. Cereb. Blood Flow Metab.* **13**: 145–152.
11. Fukuchi, T., Y. Katayama, T. Kamiya, A. McKee, F. Kashiwagi, and A. Terashi. 1998. The effect of duration of cerebral ischemia on brain pyruvate dehydrogenase activity, energy metabolites, and blood flow during reperfusion in gerbil brain. *Brain Res.* **792**: 59–65.
12. Funahashi, T., R. A. Floyd, and J. M. Carney. 1994. Age effect on brain pH during ischemia/reperfusion and pH influence on peroxidation. *Neurobiol. Aging* **15**: 161–170.
13. Gazzaley, A. H., S. J. Siegel, J. H. Kordower, E. J. Mufson, and J. H. Morrison. 1996. Circuit-specific alterations of N-methyl-D-aspartate subunit 1 in the dentate gyrus of aged monkeys. *Proc. Natl. Acad. Sci. USA* **93**: 3121–3125.
14. Geldry, S., and J. Bralet. 1994. Effect of 1,3-butanediol on cerebral energy metabolism. Comparison with β-hydroxybutyrate. *Metab. Brain Dis.* **9**: 171–181.
15. Hof, P. R., Y. E. Bogaert, R. E. Rosenthal, and G. Fiskum. 1996. Distribution of neuronal populations containing neurofilament protein and calcium-binding proteins in the canine neocortex: regional analysis and cell typology. *J. Chem. Neuroanat.* **11**: 81–98.
16. Hof, P. R., R. E. Rosenthal, and G. Fiskum. 1996. Distribution of neurofilament protein and calcium-binding proteins parvalbumin, calbindin, and calretinin in the canine hippocampus. *J. Chem. Neuroanat.* **11**: 1–12.
17. Hof, P. R., P. Vissavajhala, R. E. Rosenthal, G. Fiskum, and J. H. Morrison. 1996. Distribution of glutamate receptor subunit proteins GluR2(4), GluR5/6/7 and NMDAR1 in the canine and primate cerebral cortex: A comparative immunohistochemical analysis. *Brain Res.* **723**: 77–89.
18. Katayama, Y., and F. A. Welsh. 1989. Effect of dichloroacetate on regional energy metabolites and pyruvate dehydrogenase activity during ischemia and reperfusion in gerbil brain. *J. Neurochem.* **53**: 1817–1822.
19. Krause, G. S., D. J. DeGracia, J. M. Skjaerlund, and B. J. O'Neil. 1992. Assessment of free radical-induced damage in brain proteins after ischemia and reperfusion. *Resuscitation* **23**: 59–69.
20. Lavoie, J., and R. F. Butterworth. 1995. Reduced activities of thiamine-dependent enzymes in brains of alcoholics in the absence of Wernicke's encephalopathy. *Alcohol Clin. Exp. Res.* **19**: 1073–1077.
21. Liu, Y., R. E. Rosenthal, P. Starke-Reed, and G. Fiskum. 1993. Inhibition of post-cardiac arrest brain protein oxidation by acetyl-L-carnitine. *Free Rad. Biol. Med.* **15**: 667–670.
22. Marie, C., A. M. Bralet, and J. Bralet. 1987. Protective action of 1,3-butanediol in cerebral ischemia. A neurologic, histologic, and metabolic study. *J. Cereb. Blood Flow Metab.* **7**: 794–800.
23. Miljkovic-Lolic, M., G. Fiskum, and R. E. Rosenthal. 1997. Neuroprotective effects of acetyl-L-carnitine after stroke in rats. *Ann. Emerg. Med.* **29**: 758–765.
24. Milner, T. A., C. Aoki, K. F. R. Sheu, J. P. Blass, and V. M. Pickel. 1987. Light microscopic immunocytochemical localization of pyruvate dehydrogenase complex in rat brain: Topological distribution and relation to cholinergic and catecholaminergic nuclei. *J. Neurosci.* **7**: 171–3190.
25. Murphy, A. N., G. Fiskum, and M. F. Beal. 1999. Mitochondria in neurodegeneration: Bioenergetic function in cell life and death. *J. Cereb. Blood Flow Metab.* **19**: 231–245.
26. Oliver, C. N., P. E. Starke-Reed, E. R. Stadtman, G. J. Liu, J. M. Carney, and R. A. Floyd. 1990. Oxidative damage to brain proteins, loss of glutamine synthetase activity, and production of free radicals during ischemia/reperfusion-induced injury to gerbil brain. *Proc. Natl. Acad. Sci. USA* **87**: 5144–5147.
27. Pérez-Pinzón, M. A., P. L. Mumford, M. Rosenthal, and T. J. Sick. 1997. Antioxidants limit mitochondrial hyperoxidation and enhance electrical recovery following anoxia in hippocampal slices. *Brain Res.* **754**: 163–170.
28. Pulsinelli, W. A., J. B. Brierley, and F. Plum. 1982. Temporal profile of neuronal damage in a model of transient forebrain ischemia. *Ann. Neurol.* **11**: 491–498.
29. Radovsky, A., P. Safar, F. Sterz, Y. Lennov, H. Reich, and K. Kuboyama. 1995. Regional prevalence and distribution of ischemic neurons in dog brains 96 hours after cardiac arrest of 0 to 20 minutes. *Stroke* **26**: 2127–2134.
30. Rosenthal, M., Z. C. Feng, C. N. Raffin, M. Harrison, and T. J. Sick. 1995. Mitochondrial hyperoxidation signals residual intracellular dysfunction after global ischemia in rat neocortex. *J. Cereb. Blood Flow Metab.* **15**: 655–665.
31. Rosenthal, R. E., and G. Fiskum. 1990. Brain mitochondrial function in cerebral ischemia and resuscitation. In *Cerebral Ischemia and Resuscitation* (A. Schurr and B. M. Rigor, Eds.), pp. 289–300. CRC Press, New York.
32. Rosenthal, R. E., F. Hamud, G. Fiskum, P. J. Varghese, and S. Sharpe. 1987. Cerebral ischemia and reperfusion: prevention of brain mitochondrial injury by lidoflazine. *J. Cereb. Blood Flow Metab.* **7**: 752–758.
33. Rosenthal, R. E., R. Williams, Y. E. Bogaert, P. R. Getson, and G. Fiskum. 1992. Prevention of postischemic canine neurological

- injury through potentiation of brain energy metabolism by acetyl-L-carnitine. *Stroke* **23**: 1312–1318.
34. Sheu, K. F. R., and Y. T. Kim. 1984. Studies on bovine brain pyruvate dehydrogenase complex using antibodies against kidney enzyme complex. *J. Neurochem.* **43**: 444–449.
  35. Sheu, K. F. R., Y. T. Kim, J. P. Blass, and M. E. Weksler. 1985. An immunological study of the pyruvate dehydrogenase deficits in Alzheimer's disease brain. *Ann. Neurol.* **17**: 444–449.
  36. Sheu, K. F. R., J. C. Lai, Y. T. Kim, G. Dorante, and J. Bagg. 1985. Immunochemical characterization of pyruvate dehydrogenase complex in rat brain. *J. Neurochem.* **44**: 593–599.
  37. Sheu, K. F. R., J. P. Blass, J. M. Cedarbaum, Y. T. Kim, B. J. Harding, and J. DeCicco. 1988. Mitochondrial enzymes in hereditary ataxias. *Metab. Brain Dis.* **3**: 151–160.
  38. Shuaib, A., T. Waqar, T. Wishart, R. Kanthan, and W. Howlett. 1995. Acetyl-L-carnitine attenuates neuronal damage in gerbils with transient forebrain ischemia only when given before the insult. *Neurochem. Res.* **20**: 1021–1025.
  39. Sieber, F. E., S. C. Palmon, R. J. Traystman, and L. J. Martin. 1995. Global incomplete cerebral ischemia produces predominantly cortical neuronal injury. *Stroke* **26**: 2091–2095.
  40. Sims, N. R., and E. Zaidan. 1995. Biochemical changes associated with selective neuronal death following short-term cerebral ischaemia. *Int. J. Biochem. Cell. Biol.* **27**: 531–550.
  41. Skarkowska, L., and M. Klingenberg. 1983. On the roles of ubiquinone in mitochondria. *Biochem. J.* **338**: 674–697.
  42. Smith, M. A., M. Rudnicka-Nawrot, P. L. Richey, D. Praprotnik, P. Mulvihill, C. A. Miller, L. M. Sayre, and G. Perry. 1995. Carbonyl-related posttranslational modification of neurofilament protein in the neurofibrillary pathology of Alzheimer's disease. *J. Neurochem.* **64**: 2660–2666.
  43. Sorbi, S., E. D. Bird, and J. P. Blass. 1983. Decreased pyruvate dehydrogenase complex activity in Huntington and Alzheimer brain. *Ann. Neurol.* **13**: 72–78.
  44. Stadtman, E. R. 1990. Covalent modification reactions are marking steps in protein turnover. *Biochemistry* **10**: 6323–6331.
  45. Tabatabaie, T., J. D. Potts, and R. A. Floyd. 1996. Reactive oxygen species-mediated inactivation of pyruvate dehydrogenase. *Arch. Biochem. Biophys.* **336**: 290–296.
  46. Zaidan, E., and N. R. Sims. 1993. Selective reductions in the activity of the PDH complex in mitochondria isolated from brain subregions following forebrain ischemia in rats. *J. Cereb. Blood Flow Metab.* **13**: 98–104.
  47. Zaidan, E., and N. R. Sims. 1997. Reduced activity of the pyruvate dehydrogenase complex but not cytochrome c oxidase is associated with neuronal loss in the striatum following short-term forebrain ischemia. *Brain Res.* **772**: 23–28.
  48. Zaidan, E., K. F. R. Sheu, and N. R. Sims. 1998. The pyruvate dehydrogenase complex is partially inactivated during early recirculation following short-term forebrain ischemia in rats. *J. Neurochem.* **70**: 233–241.